Some Properties of Gyrostats Dynamical Regimes close to New Strange Attractors of the Newton-Leipnik Type

Anton V. Doroshin

Space Engineering Department (Division of Flight Dynamics and Control Systems), Samara National Research University, Samara, Russia (doran@inbox.ru; doroshin@ssau.ru)

Abstract New dynamical systems with strange attractors are numerically investigated in the article. These dynamical systems correspond to the main mathematical model describing the attitude dynamics of multi-spin spacecraft and gyrostat-satellites. The considering dynamical systems are structurally related to the well-known Newton-Leipnik system. Properties of the strange attractors arising inside the phase spaces of the dynamical systems are examined with the help of the numerical modelling.

Introduction

The investigation of dynamical systems with strange attractors is one of the important problems of the modern nonlinear dynamics [1-19]. Especially interesting cases of such systems represent the dynamical systems describing the natural behavior of mechanical, electrodynamical, biological, meteorological and other systems.

As the important part of such mechanical systems it is possible to indicate the multi-body systems, which dynamics is described by the ordinal differential equations. As one of the partial cases of such multi-body systems, in this paper we consider the mechanical model of the multi-spin spacecraft (MSSC), also called as the gyrostat-satellite. As it was shown in previous works [e.g.1-5], the corresponding phase space of differential equations of the MSSC attitude dynamics can contain different forms of strange attractors, including cases of Newton-Leipnik-like two-scroll strange attractors [6]. Moreover, in the framework of MSSC dynamics the strange chaotic attractors can be defined as one additional dynamical opportunity, which allows to solve the task of the spacecraft spatial reorientation using chaotic properties of its angular motion (that is quite actual in some nontrivial cases of spacecraft motion, including accidents/failures in main control systems) [3-5]. Therefore, the problem of the strange attractors examination is important not

Y. Bi et al. (eds.), Intelligent Systems and Applications,
Studies in Computational Intelligence 751

only from the mathematical point of view, but also from the side of possible technical applications.

In this work we use the MSSC equations of motion as a mathematical basis which allows to write and to investigate the dynamical systems in the form of three ordinal differential equations containing strange chaotic attractors of the Newton-Leipnik type.

Main dynamical systems

The MSSC [1-5] represents the multi-body mechanical system with conjugated pairs of rotors placed on the inertia principle axes of the main body (fig.1).

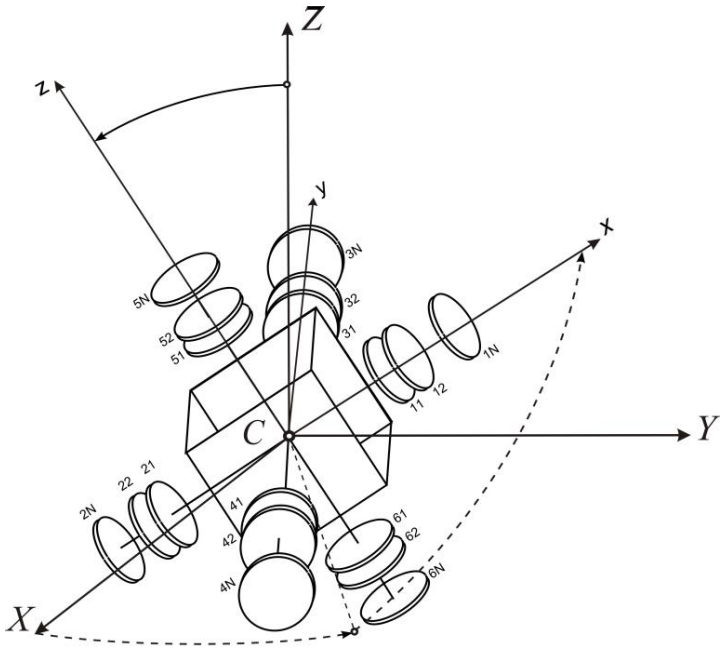

Fig. 1. The MSSC as the multirotor system

The equations of angular motion of MSSC around the "fixed" point O (the center of mass) [1-5] can be presented in the form:

$$\begin{cases} \hat{A}\dot{p} + \dot{D}_{12} + \left(\hat{C} - \hat{B}\right)qr + \left[qD_{56} - rD_{34}\right] = M_x^e; \\ \hat{B}\dot{q} + \dot{D}_{34} + \left(\hat{A} - \hat{C}\right)rp + \left[rD_{12} - pD_{56}\right] = M_y^e; \\ \hat{C}\dot{r} + \dot{D}_{34} + \left(\hat{B} - \hat{A}\right)pq + \left[pD_{34} - qD_{12}\right] = M_z^e \end{cases} \tag{1}$$

In these equations the following notations are used: $\boldsymbol{\omega}=[p, q, r]^{\mathrm{T}}$ – the vector of

the absolute angular velocity of the MSSC main body (in projections on the connected frame $Oxyz$); $\hat{A}, \hat{B}, \hat{C}$ are the summarized moments of inertia of the MSSC; $M_x^e, M_y^e\ M_z^e -$ the external torques acting on the system. The summarized rotors' angular momentums in the considered case are formed by the control system in the shape:

$$D_{12} = \alpha_p p + \alpha_0;\ D_{34} = \beta_q q + \beta_0;\ \ D_{56} = \gamma_r r + \gamma_0, \tag{2}$$

The "external" torques also are created (by thrusters) as follows:

$$M_x^e = m_x + \alpha_1 p;\ \ M_y^e = m_y + \beta_1 q;\ \ M_z^e = m_z + \gamma_1 r, \tag{3}$$

In purposes of the fully description of the attitude dynamics of MSSC the dynamical system (3) should be supplemented by the kinematic equations for Euler (Tait–Bryan) angles defining the rotation of the MSSC connected system $Oxyz$ around the "fixed" point O (the mass center) and relatively the inertial coordinates system $OXYZ$:

$$\begin{cases} \dot{\gamma} = p\sin\varphi + q\cos\varphi; \\ \dot{\psi} = \dfrac{1}{\cos\gamma}\left(p\cos\varphi - q\sin\varphi\right); \\ \dot{\varphi} = r - \dfrac{\sin\gamma}{\cos\gamma}\left(p\cos\varphi - q\sin\varphi\right). \end{cases} \tag{4}$$

So, as we can see from the dynamical equations (1) (with the definitions (2) and (3)), the following constant "controlling" terms/coefficients take place: $\left\{\alpha_0, \beta_0, \gamma_0, m_x, m_y, m_z, \alpha_1, \beta_1, \gamma_1, \alpha_p, \beta_q, \gamma_r\right\} \sim \text{const}$

The system (1) in addition of (2) and (3) can be rewritten in the form of differential equations with quadratic right parts:

$$\begin{cases} \dot{x} = a_0 + a_1 x + a_2 y + a_3 z + a_4 x^2 + a_5 y^2 + a_6 z^2 + a_7 xy + a_8 xz + a_9 yz; \\ \dot{y} = b_0 + b_1 x + b_2 y + b_3 z + b_4 x^2 + b_5 y^2 + b_6 z^2 + b_7 xy + b_8 xz + b_9 yz; \\ \dot{z} = c_0 + c_1 x + c_2 y + c_3 z + c_4 x^2 + c_5 y^2 + c_6 z^2 + c_7 xy + c_8 xz + c_9 yz; \end{cases} \tag{5}$$

where $Coeff = \left\{a_i, b_i, c_i\right\}_{0 \le i \le 9} \in \mathbb{R}^{30}$ is the set of constant parameters, and where the designation of the variables are used: $p = x;\ q = y;\ r = z.$ The following coefficients [1] of the system (5) have exact values:

$$\begin{cases} a_0 = \dfrac{m_x}{\hat{A}+\alpha_p}; \;\; b_0 = \dfrac{m_y}{\hat{B}+\beta_q}; \;\; c_0 = \dfrac{m_z}{\hat{C}+\gamma_r}; \\ a_1 = \dfrac{\alpha_1}{\hat{A}+\alpha_p}; \quad b_1 = \dfrac{\gamma_0}{\hat{B}+\beta_q}; \quad c_1 = \dfrac{-\beta_0}{\hat{C}+\gamma_r}; \\ a_2 = \dfrac{-\gamma_0}{\hat{A}+\alpha_p}; \quad b_2 = \dfrac{\beta_1}{\hat{B}+\beta_q}; \quad c_2 = \dfrac{\alpha_0}{\hat{C}+\gamma_r}; \\ a_3 = \dfrac{\beta_0}{\hat{A}+\alpha_p}; \quad b_3 = \dfrac{-\alpha_0}{\hat{B}+\beta_q}; \quad c_3 = \dfrac{\gamma_1}{\hat{C}+\gamma_r}; \\ a_4 = a_5 = a_6 = b_4 = b_5 = b_6 = c_4 = c_5 = c_6 \equiv 0; \\ a_7 = 0; \;\; b_7 = 0; \;\; c_7 = \left(\hat{A}-\hat{B}-\beta_q+\alpha_p\right)\Big/\left(\hat{C}+\gamma_r\right); \\ a_8 = 0; \;\; b_8 = \left(\hat{C}-\hat{A}-\alpha_p+\gamma_r\right)\Big/\left(\hat{B}+\beta_q\right); \; c_8 = 0; \\ a_9 = \left(\hat{B}-\hat{C}-\gamma_r+\beta_q\right)\Big/\left(\hat{A}+\alpha_p\right); \;\; b_9 = 0; \; c_9 = 0. \end{cases} \tag{6}$$

So, taking into our consideration correspondences (6) connecting the dynamical system's coefficients $\{a_i, b_i, c_i\}$ and MSSC parameters $\{\alpha_p, \alpha_0, m_x, \alpha_1, \beta_q, \beta_0, m_y, \beta_1, \gamma_r, \gamma_0, m_z, \gamma_1\}$ with predefined inertia moments $\{\hat{A}, \hat{B}, \hat{C}\}$, it is possible to find the concrete numerical values of the constants from the set

$$Control = \{\alpha_p, \alpha_0, m_x, \alpha_1, \beta_q, \beta_0, m_y, \beta_1, \gamma_r, \gamma_0, m_z, \gamma_1\} \in \mathbb{R}^{12} \tag{7}$$

which can be used to providing the appropriate values of the coefficients $\{a_i, b_i, c_i\}$ close to a "target system" with a strange attractor. Due to the incompatibility of the indicated sets *Coeff* and *Control* we cannot solve this task exactly (as the algebraic equations), therefore, to obtain these values we must use some additional algorithms, e.g. the gradient-search method [3, 5]. Then using the algorithm [1] taking the Newton-Leipnik system as the "target system", it is possible to obtain new concretized dynamical systems with strange attractors inside phase spaces. These new systems and the corresponding properties are presented in the next section of this article.

The numerical investigation of new strange attractors

In this section we focus on the numerical investigation of the dynamical systems for MSSC obtained in the work [1]. These systems contain strange chaotic attractors and/or have the regular but very complex dynamical behavior, that is important not only from the mathematical point of view, but also from the technical point of practical applications. The next subsections of the article present the corresponding

blocks of the numerical modeling for itch dynamical system of the Newton-Leipnik type which were found in [1] and [5].

Here it is important to remind [6] the structure of the classical Newton-Leipnik system (NL). For the NL equations the following coefficients take place (all other coefficients equal to zero):

$$NL = \begin{Bmatrix} a_1 = -0.4;\ a_2 = 1;\ a_9 = 10; \\ b_1 = -1;\ b_2 = -0.4;\ b_8 = 5; \\ c_3 = 0.175;\ c_7 = -5 \end{Bmatrix} \tag{8}$$

In the NL-system two strange attractors exist (fig.2): the upper attractor (black) with initial states (0.349, 0, −0.16), and the lower attractor (blue) with initial states (0.349, 0, −0.18).

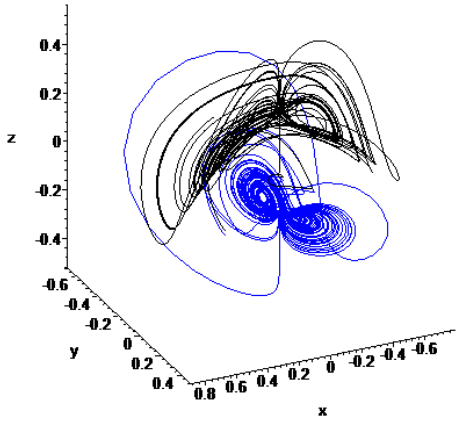

Fig. 2. The classical *Newton-Leipnik* attractors

So, below in the next subsections six new cases of the dynamical systems of the NL-type will be described, which are called as “SysA”, “SysB”, “SysC”, “SysD”, “Complex1” and “Complex2”.

The system SysA analysis

As it was explored in [1], the dynamical system with new strange attractor can be built at the following concretized set *Coeff* of non-zero numerical coefficients:

$$SysA = \begin{Bmatrix} a_1 = -0.4000;\ a_2 = 1.0738;\ a_9 = 10.0403; \\ b_1 = -0.0864;\ b_2 = -0.2471;\ b_8 = 0.1118; \\ c_3 = 0.1752;\ c_7 = -4.7831 \end{Bmatrix} \tag{9}$$

These coefficients correspond to the following MSSC parameters [1]:

$$\hat{A} = 1000; \quad \hat{B} = 2500; \quad \hat{C} = 3000 \ [\text{kg}\cdot\text{m}^2];$$

$$Control\_SysA = \left(\alpha_p, \alpha_0, m_x, \alpha_1, \beta_q, \beta_0, m_y, \beta_1, \gamma_r, \gamma_0, m_z, \gamma_1\right) =$$

$$= \left(-692.7387,\ 0,\ 0,\ -122.9331,\ 1319.2399,\ 0,\ 0,\right.$$

$$\left.-943.7322,\ -2265.7542,\ -329.9222,\ 0,\ 128.6660\right).$$

Then the new system takes place:

$$SysA = \begin{cases} \dot{x} = -0.4000x + 1.0738y + 10.0403yz; \\ \dot{y} = -0.0864x - 0.2471y + 0.1118xz; \\ \dot{z} = 0.1752z - 4.7831xy \end{cases} \tag{10}$$

The SysA has a new strange chaotic attractor (fig. 3) at the initial values $x(0) = 0.05;\ y(0) = 0.1;\ z(0) = 1.5.$ This strange attractor (red) is depicted (fig.3) together with the classical "upper" Newton-Leipnik attractor (black).

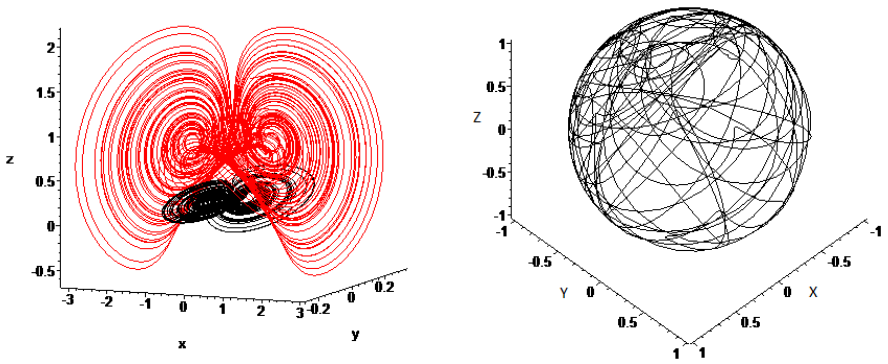

Fig. 3. The *SysA* attractor (red), the *Newton-Leipnik* attractor (black) and the $\mathbf{e}_z$-hodograph

The figure (fig.3) also contain the co-called hodograph ($\mathbf{e}_z$-hodograph) which represents the space curve corresponding to the trajectory motion of the apex of the *Oz*-axis of the MSSC (fig.1) in the inertial space *OXYZ*, that characterizes the chaotic side of the angular motion of the spacecraft.

In the purposes of the chaotic aspects description of the SysA-system dynamics along its strange attractor, we can present the time-history (fig.4) of the spatial angles (4), the Lyapunov's exponents for the SysA strange attractor and the fast Fourier transform (FFT) spectrum (fig.5) for the $x(t)$-signal on the attractor.

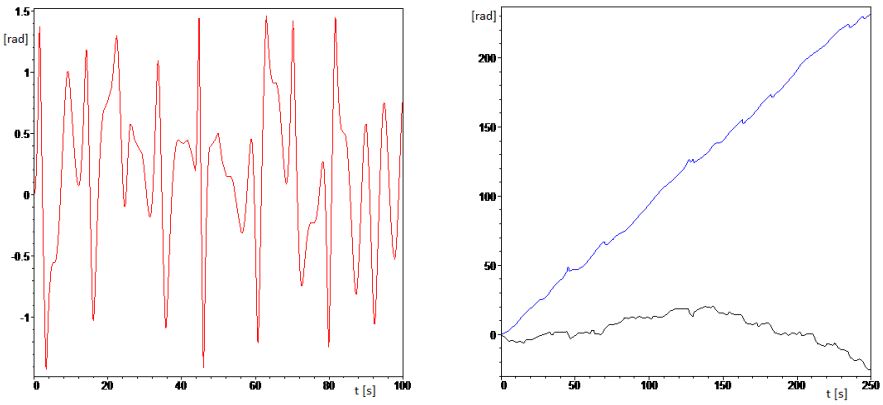

Fig. 4. The time-history of the angle $\gamma(t)$ (red), $\psi(t)$ (black), $\varphi(t)$ (blue) in the *SysA* system

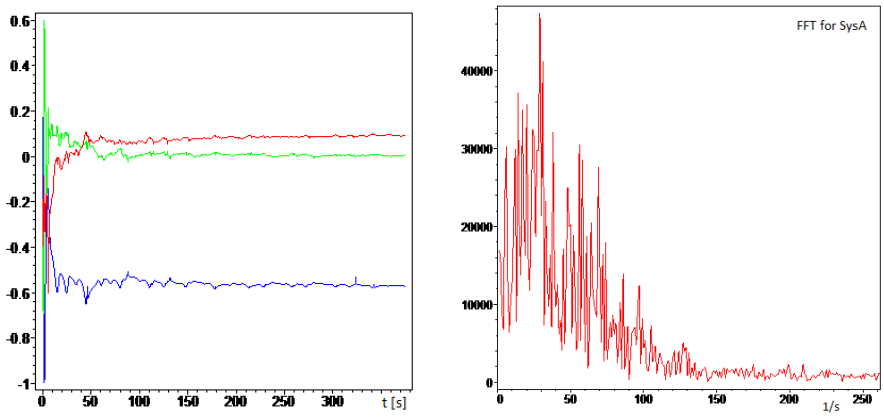

Fig. 5. The Lyapunov exponents and the spectrum of the fast Fourier transform of the $x(t)$-signal

It is important to calculate the Lyapunov's exponents spectrum and the Kaplan-Yorke dimension D_{KY} for the SysA strange attractor (evaluated with the tolerance 10^{-2}):

$$\{\lambda_1 = 0.09; \lambda_2 = 0.00; \lambda_3 = -0.57\}; \quad D_{KY} = 2.17$$

As can we see, the Lyapunov's exponents spectrum has the classical signature for strange attractor in 3D-system {+,0,-}; the the Kaplan-Yorke dimension is fractional, and the FFT-spectrum is complex (with non-zero "continuous" amplitudes). All of these notations are the typical properties for chaotic strange attractors.

Also it is quite illustrative to show the Poincaré sections for SysA strange attractor (fig.6-8), that also confirms the fractal nature of the strange attractor.

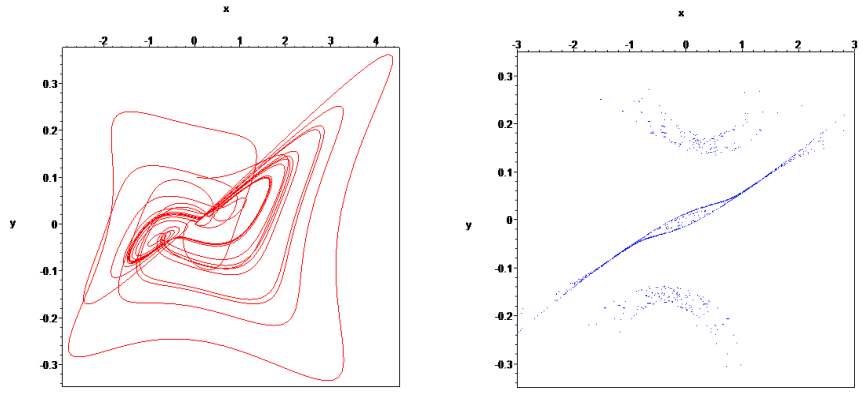

Fig. 6. The xy-projection of *SysA* strange attractor and its Poincaré section (by the plane z=1)

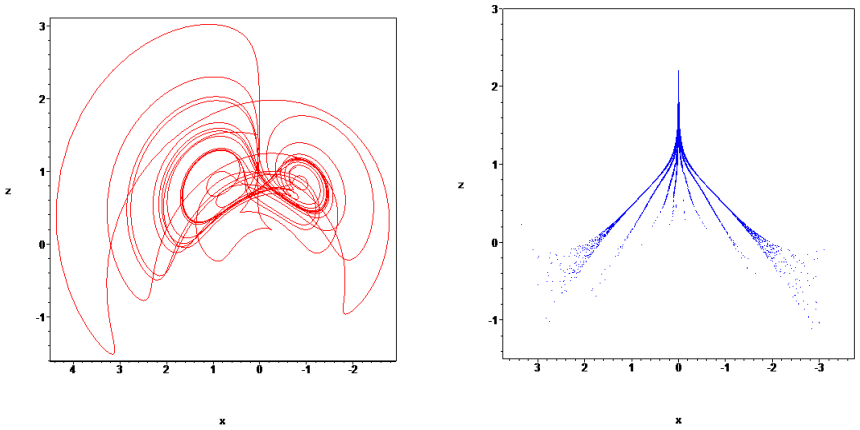

Fig. 7. The xz-projection of *SysA* strange attractor and its Poincaré section (by the plane y=0)

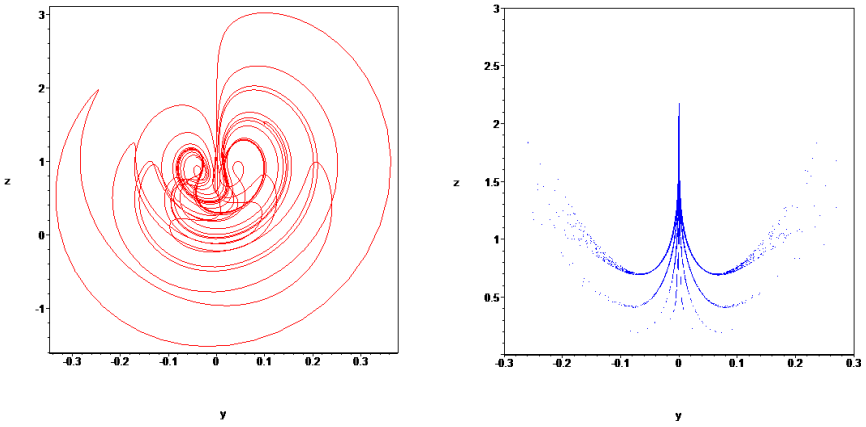

Fig. 8. The yz-projection of *SysA* strange attractor and its Poincaré section (by the plane x=0)

The system SysB analysis

The second case of the MSSC motion with generating the strange attractor realizes at the following parameters [1]:

$$\begin{aligned}
&\hat{A} = 1000;\ \ \hat{B} = 2500;\ \ \hat{C} = 3000\ [\mathrm{kg}\cdot\mathrm{m}^2];\\
&Control_SysB = \left(\alpha_p, \alpha_0, m_x, \alpha_1, \beta_q, \beta_0, m_y, \beta_1, \gamma_r, \gamma_0, m_z, \gamma_1\right) =\\
&= \left(-695.9057,\ 0,\ 0,\ -121.5977,\ 1281.2392,\ 0,\ 0,\right.\\
&\left.-1467.3693,\ -2272.0667,\ -326.3300,\ 0,\ 199.3635\right);
\end{aligned} \tag{11}$$

Then the dynamical system SysB can be indicated with corresponding coefficients:

$$SysB = \left\{\begin{array}{l} a_1 = -0.3999;\ a_2 = 1.0731;\ a_9 = 10.0407; \\ b_1 = -0.0863;\ b_2 = -0.3881;\ b_8 = 0.1121; \\ c_3 = 0.2739;\ c_7 = -4.7767 \end{array}\right\} \tag{12}$$

So we have the new dynamical system

$$SysB = \left\{\begin{array}{l} \dot{x} = -0.3999x + 1.0731y + 10.0407yz; \\ \dot{y} = -0.0863x - 0.3881y + 0.1121xz; \\ \dot{z} = 0.2739z - 4.7767xy \end{array}\right. \tag{13}$$

with the strange chaotic attractor (fig. 9) at the initial values $x(0) = 0.05;\ y(0) = 0.1;\ z(0) = 1.5,$ depicted together with the "upper" Newton-Leipnik attractor.

In this case the Lyapunov's exponents spectrum and the Kaplan-Yorke dimension D_{KY} for the SysA strange attractor (evaluated with the tolerance 10^{-2}) are:

$$\left\{\lambda_1 = 0.14; \lambda_2 = 0.00; \lambda_3 = -0.61\right\};\quad D_{KY} = 2.22$$

As in the previous case, we see the typical properties for chaotic strange attractors: the Lyapunov's exponents spectrum has the classical signature for strange attractor in 3D-system {+,0,-}; the the Kaplan-Yorke dimension is fractional, and the FFT-spectrum (fig.11) is complex (with non-zero "continuous" amplitudes). The Poincaré sections for SysB strange attractor (fig.12-14) confirm the fractal nature of the strange attractor.

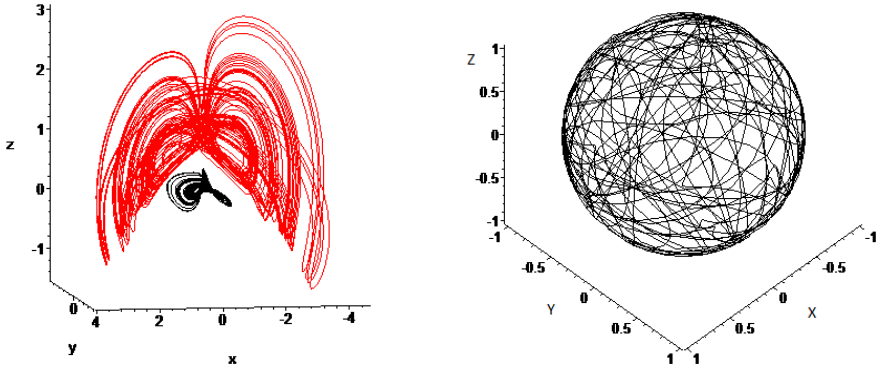

Fig. 9. The *SysB* attractor (red), the *Newton-Leipnik* attractor (black) and the $\mathbf{e}_z$-hodograph

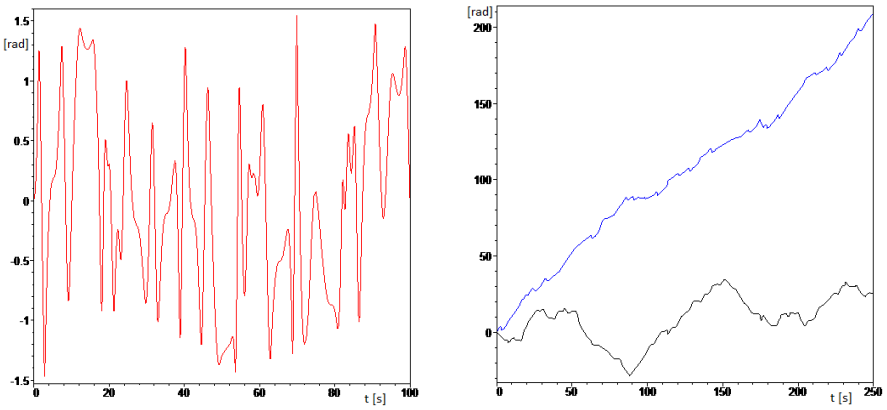

Fig. 10. The time-history of the angle $\gamma(t)$ (red), $\psi(t)$ (black), $\varphi(t)$ (blue) in the *SysB* system

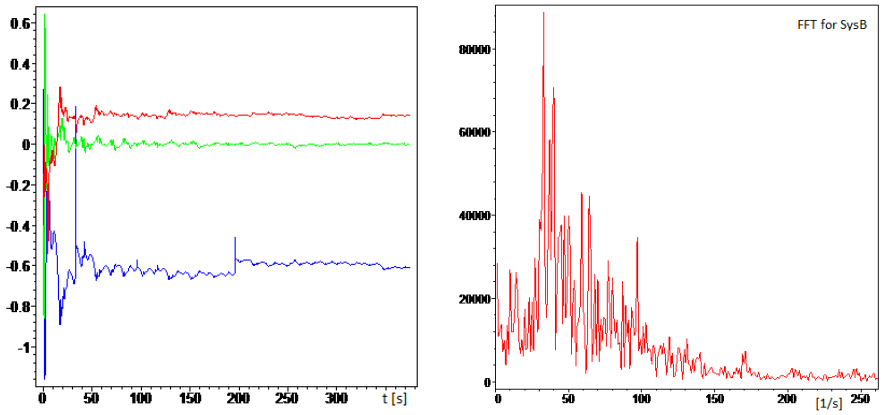

Fig. 11. The Lyapunov exponents and the spectrum of the fast Fourier transform of $x(t)$-signal

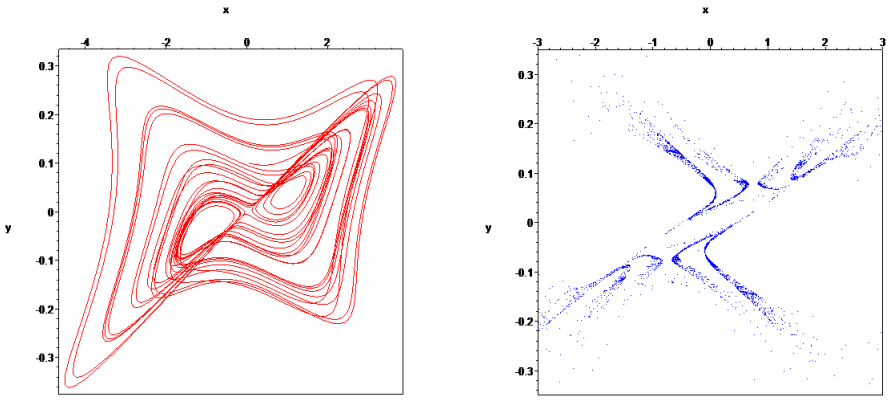

Fig. 12. The xy-projection of *SysB* strange attractor and its Poincaré section (by the plane z=1)

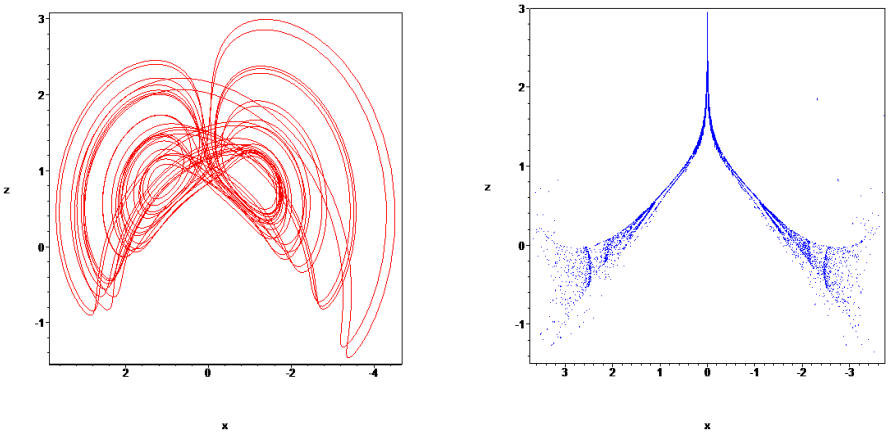

Fig. 13. The xz-projection of *SysB* strange attractor and its Poincaré section (by the plane y=0)

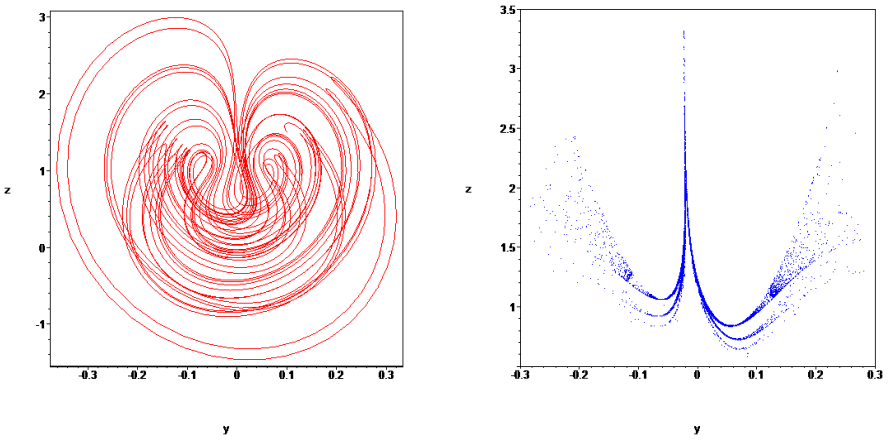

Fig. 14. The yz-projection of *SysB* strange attractor and its Poincaré section (the plane x=-0.25)

The system SysC analysis

The MSSC has the complex attitude dynamics at the realization of the following parameters [1]:

$$\hat{A} = 1000; \quad \hat{B} = 2500; \quad \hat{C} = 3000 \ [\text{kg}\cdot\text{m}^2];$$

$$Control\_SysC = \left(\alpha_p, \alpha_0, m_x, \alpha_1, \beta_q, \beta_0, m_y, \beta_1, \gamma_r, \gamma_0, m_z, \gamma_1\right) =$$

$$= \left(-682.4176,\ 0,\ 0,\ -126.8955,\ 1451.8728,\ 0,\ 0,\right.$$

$$\left.-1473.7799,\ -2237.0650,\ -340.5281,\ 0,\ 292.1299\right);$$

Then the corresponding dynamical system can be presented:

$$SysC = \begin{cases} \dot{x} = -0.3996x + 1.0723y + 10.0413yz; \\ \dot{y} = -0.0862x - 0.3729y + 0.1127xz; \\ \dot{z} = 0.3829z - 4.7636xy \end{cases} \tag{14}$$

At the initial values $\{x(0) = 0.05;\ y(0) = 0.1;\ z(0) = 1.5\}$ the system has the phase trajectory (fig.15) similar to the previous strange attractor's form (e.g. fig.3,9) – this complex form was the main reason to define this dynamical system as the system with strange attractor in [1]. However, at the more detailed investigation of this system the fact of its regularity was confirmed. As can we see, firstly, the regular limit cycle (fig.15-black) is contained inside the phase trajectory; secondly, the regular Lyapunov's exponents take place with the corresponding integer dimension of the attractor (the limit cycle in the form of the 3D-closed-curve): $\{\lambda_1 = 0.00; \lambda_2 = -0.11; \lambda_3 = -0.28\}$; $D_{KY} = 1$. Also the simple (discrete and concentrated) FFT-spectrum is actual for this regular attractor.

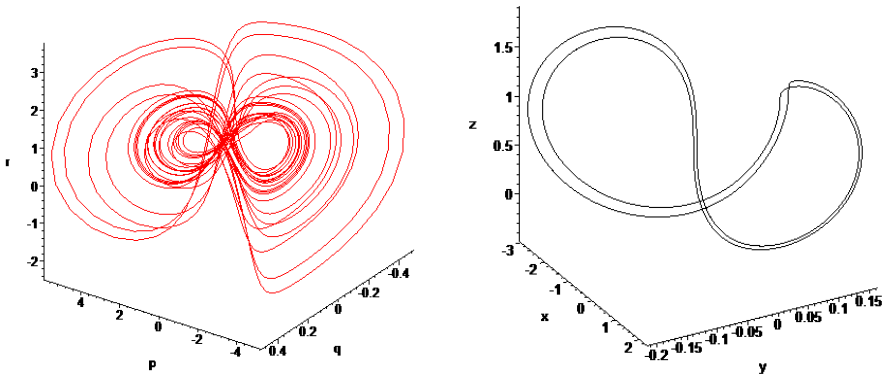

Fig. 15. The phase trajectory (red) close to the limit cycle of the *SysC* system (black)

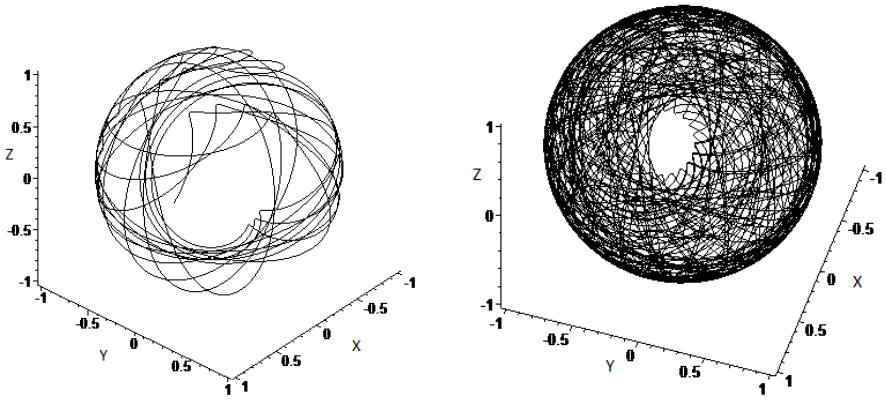

Fig. 16. The $\mathbf{e}_z$-hodograph (and its evolution) of the system *SysC*

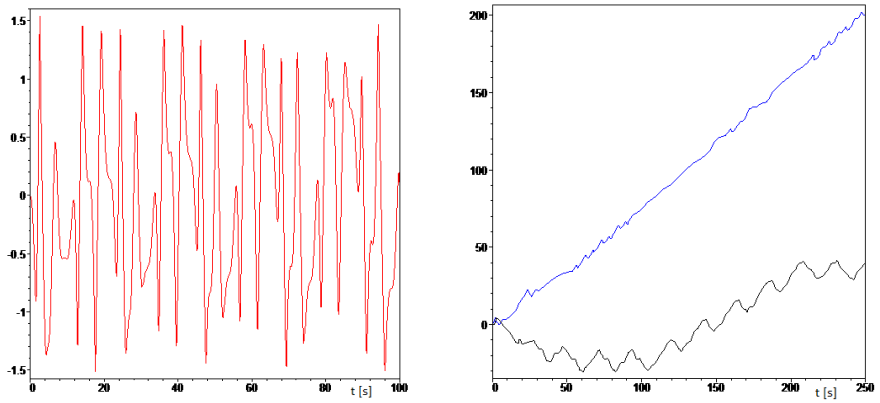

Fig. 17. The time-history of the angle $\gamma(t)$ (red), $\psi(t)$ (black), $\varphi(t)$ (blue) in the *SysC* system

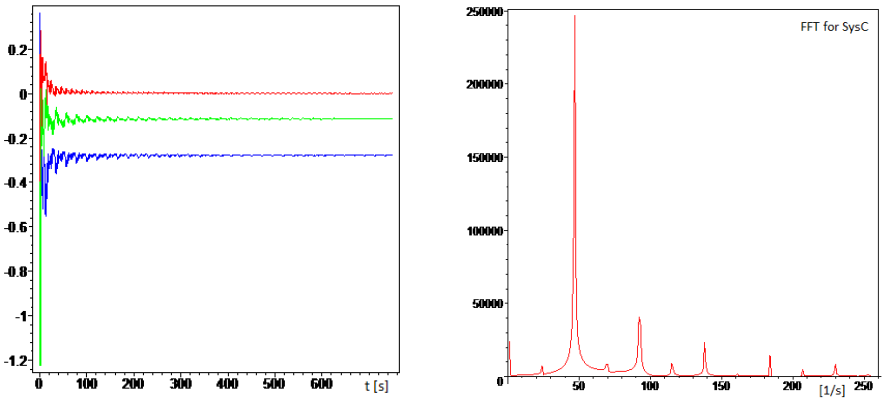

Fig. 18. The Lyapunov exponents and the spectrum of the fast Fourier transform of $x(t)$-signal

The system SysD

In the work [5] one more dynamical system with strange attractor was found at the following MSSC parameters:

$$\hat{A} = 90;\ \hat{B} = 70;\ \hat{C} = 50[\mathrm{kg}\cdot\mathrm{m}^2];$$
$$Control\_SysD = \left\{ \begin{array}{l} \alpha_p = \text{-}80.6893;\ \alpha_0 = 0;\ m_x = 0;\ \alpha_1 = \text{-}3.7243; \\ \beta_q = 45.7309;\ \beta_0 = 0;\ m_y = 0;\ \beta_1 = \text{-}46.2952; \\ \gamma_r = \text{-}27.7522;\ \gamma_0 = \text{-}9.9951;\ m_z = 0;\ \gamma_1 = 3.8934 \end{array} \right\} \quad (15)$$

As the result, the dynamical system took the form:

$$SysD = \left\{ \begin{array}{l} \dot{x} = -0.4x + 1.0735y + 10.0403yz; \\ \dot{y} = -0.0864x - 0.4y + 0.1118xz; \\ \dot{z} = 0.1750z - 4.7834xy \end{array} \right. \quad (16)$$

The detailed investigation of the strange attractor (Fig.19) in this system confirmed the presence of all properties, which are usual for chaotic fractal objects: the Lypunov's spectrum $\{\lambda_1 = 0.10; \lambda_2 = 0.00; \lambda_3 = -0.59\}$ has the strange attractor's signature {+,0,-}; the fractional dimension $D_{KY} = 2.16$; the complex FFT-spectrum (fig.21) and fractal pictures at the Poincaré sections (fig.22-24).

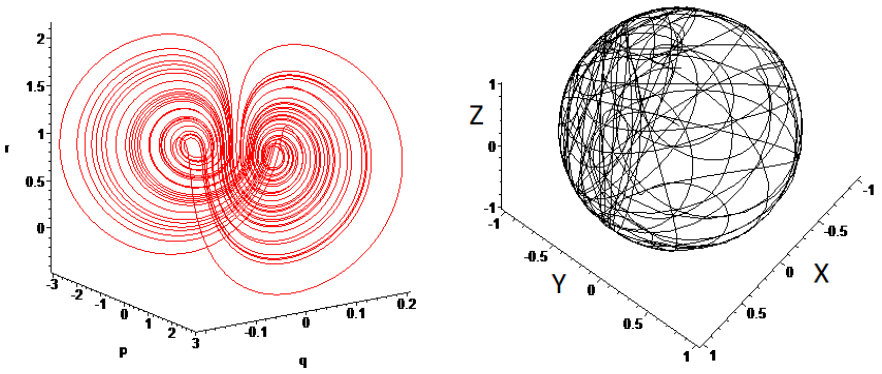

Fig. 19. The phase trajectory (red) and $\mathbf{e}_z$-hodograph (black) for the *SysD* system

The chaotic angular motion of the MSSC also is illustrated by the complex $\mathbf{e}_z$-hodograph of the *Oz*-axis apex (fig.19), and by the chaotic time-evolutions for the Euler angles (fig.20).

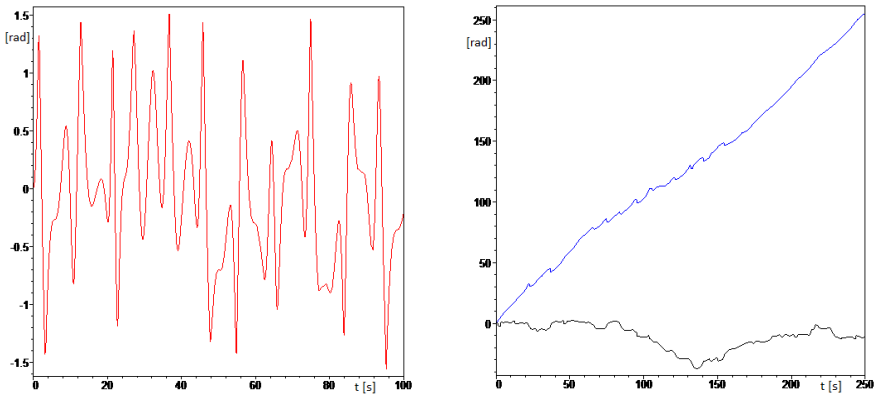

Fig. 20. The time-history of the angle $\gamma(t)$ (red), $\psi(t)$ (black), $\varphi(t)$ (blue) in the *SysD* system

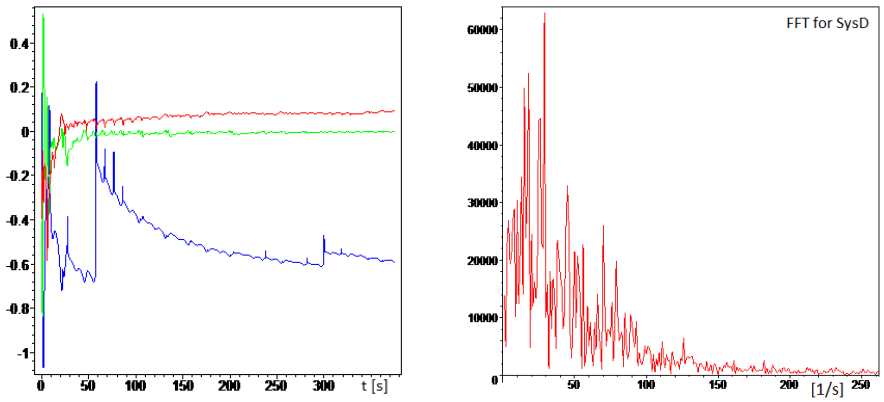

Fig. 21. The Lyapunov exponents and the spectrum of the fast Fourier transform of $x(t)$-signal

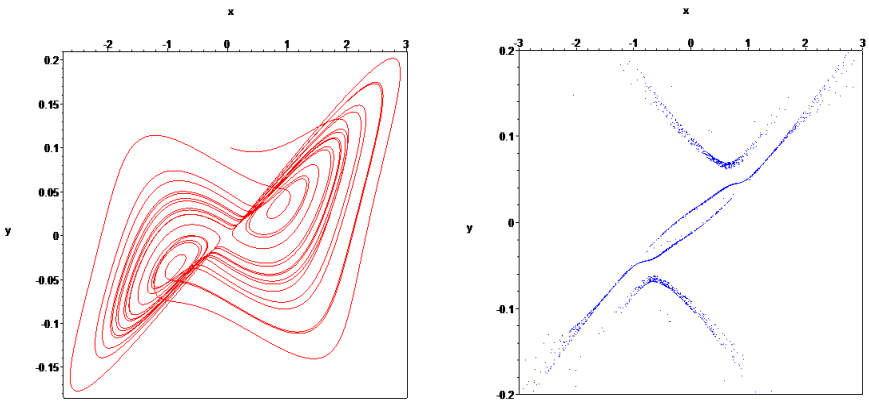

Fig. 22. The xy-projection of *SysD* strange attractor and its Poincaré section (by the plane z=1)

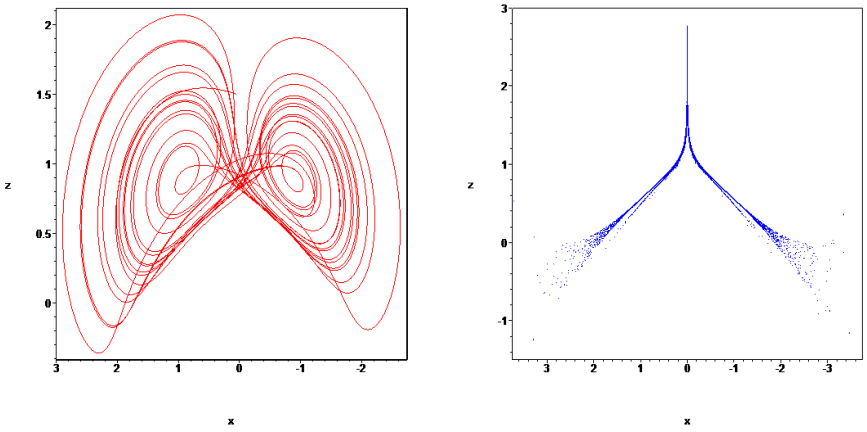

Fig. 23. The xz-projection of *SysD* strange attractor and its Poincaré section (by the plane y=0)

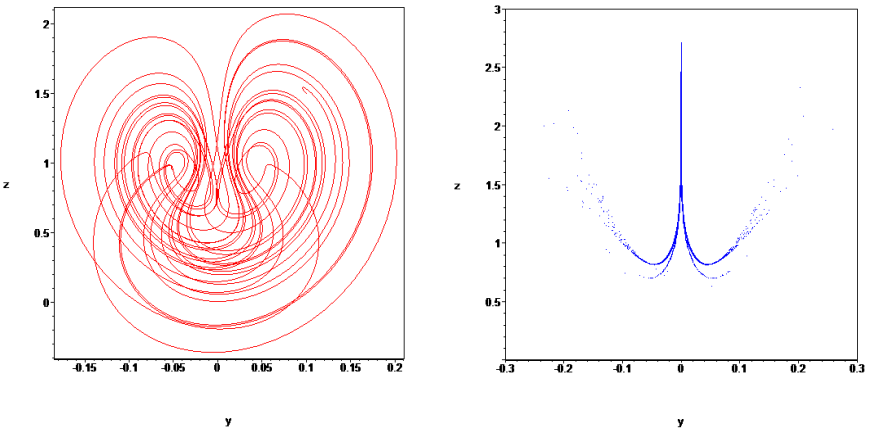

Fig. 24. The yz-projection of *SysD* strange attractor and its Poincaré section (by the plane x=0)

The system Complex1

In this section we consider the system which do not include the strange attractors, but it has the complex dynamics of phase trajectories, that can be close to the chaotic dynamics in the sense of a complexity of the MSSC angular motion.
In this case the MSSC has the following parameters [1]:

$$\begin{aligned}
&\hat{A}=100;\quad \hat{B}=250;\quad \hat{C}=300\ [\mathrm{kg}\cdot\mathrm{m}^2];\\
&Control_Complex1=\left(\alpha_p,\alpha_0,m_x,\alpha_1,\beta_q,\beta_0,m_y,\beta_1,\gamma_r,\gamma_0,m_z,\gamma_1\right)=\\
&=\left(-2886.4968,\ 0,\ 0,\ 361.7618,\ 409.0296,\ 0,\ 0,-263.7884,\right.\\
&\left.467.3039,-476.9110,\ 0,\ 133.8367\right);
\end{aligned}\tag{17}$$

Then the dynamical system can be written:

$$Complex1 = \begin{cases} \dot{x} = -0.1298x - 0.1712y + 0.03886yz; \\ \dot{y} = -0.7237x - 0.4003y + 5.3925xz; \\ \dot{z} = 0.1744z - 4.4904xy \end{cases} \tag{18}$$

In the considered case the complex phase trajectory is generated in the system; and this phase trajectory in the stream of time proceeds to the limit cycle depicted at the figure (fig.25).

As it is evaluated for the indicated regular attractor (limit cycle), the Lyapunov exponents spectrum $\{\lambda_1 = 0.00; \lambda_2 = -0.09; \lambda_3 = -0.28\}$ has the signature {0,-,-}; the dimensions is integer D_{KY}=1; the FFT-spectrum (fig.27) is simple, concentrated. The $\mathbf{e}_z$-hodograph in this case is regularized (fig.26).

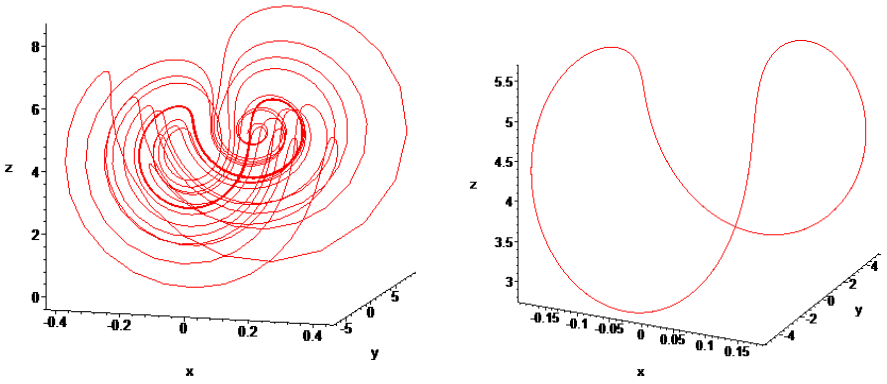

Fig. 25. The phase trajectory of the *Complex1*-system and its limit cycle

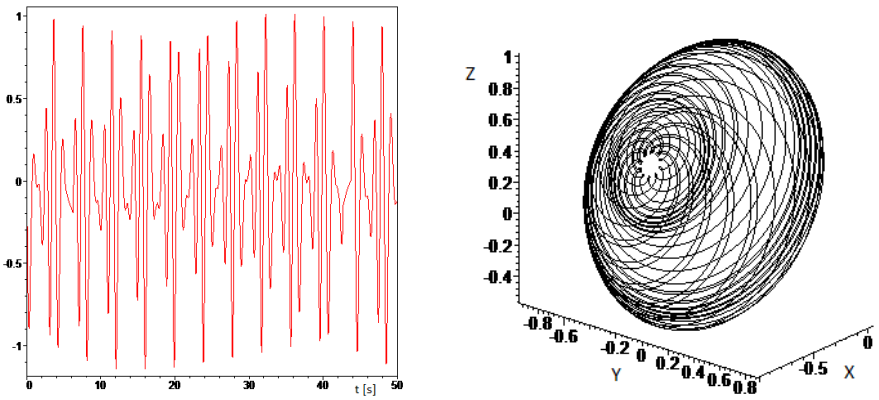

Fig. 26. The time-history of the angle $\gamma(t)$ and $\mathbf{e}_z$-hodograph (black) for the *Complex1* system

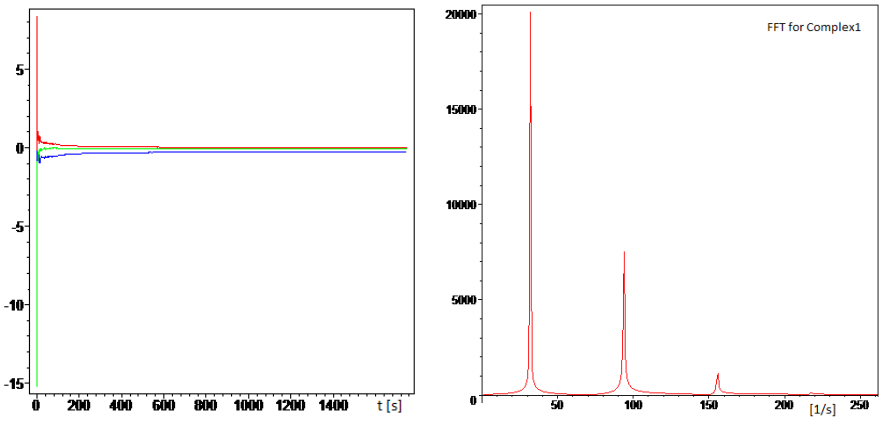

Fig. 27. The Lyapunov exponents and the spectrum of the fast Fourier transform of $x(t)$-signal

The system Complex2

At the end of the considering set of dynamical systems with complicated dynamics let us present the Complex2 system, which is realized at the MSSC parameters [1]:

$$\begin{aligned}&\hat{A}=100;\quad \hat{B}=250;\quad \hat{C}=300\ [\mathrm{kg}\cdot\mathrm{m}^2];\\ &Control\_Complex2=\left(\alpha_p,\alpha_0,m_x,\alpha_1,\beta_q,\beta_0,m_y,\beta_1,\gamma_r,\gamma_0,m_z,\gamma_1\right)=\\ &=\left(-2947.8679,\ 0,\ 0,\ 23.5201,\ 430.1965,\ 0,\ 0,\right.\\ &\left.-77.3623,\ 500.7775,-105.2338,\ 0,\ 38.9642\right);\end{aligned} \tag{19}$$

$$Complex2=\begin{cases}\dot{x}=-0.0083x-0.0369y+0.0423yz;\\ \dot{y}=-0.1547x-0.1137y+5.3641xz;\\ \dot{z}=0.0487z-4.4058xy\end{cases} \tag{20}$$

Then in the system's phase space the complex objet is contained; this object can be defined as the complex periodical cycle (fig.28, 31) with two alternate dissipative scrolls. At the figure (fig.31) this complex periodical cycle is depicted separately (at the initial values $x(0)=0.1$, $y(0)=0.0$, $z(0)=0.0$). Evaluations give the non-negative Lyapunov exponents $\{\lambda_1=3.45;\lambda_2=0.36;\lambda_3=0.00\}$ for the indicated cycle; and it means the exponential instability of this regime and increasing the phase volume along this complex cycle. Moreover, the dynamical complexity of the regime can be illustrated by the quite complicated FFT-spectrum (fig.30), which is rather distributed than concentrated, but decaying. The angular motion of the MSSC is in this case is complex and practically chaotic, that confirmed by the complex hodograph (fig.28).

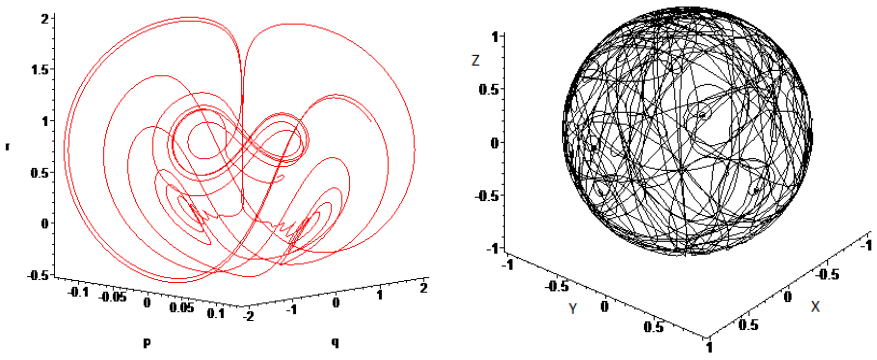

Fig. 28. The *Complex2* phase trajectory (red) and $\mathbf{e}_z$-hodograph

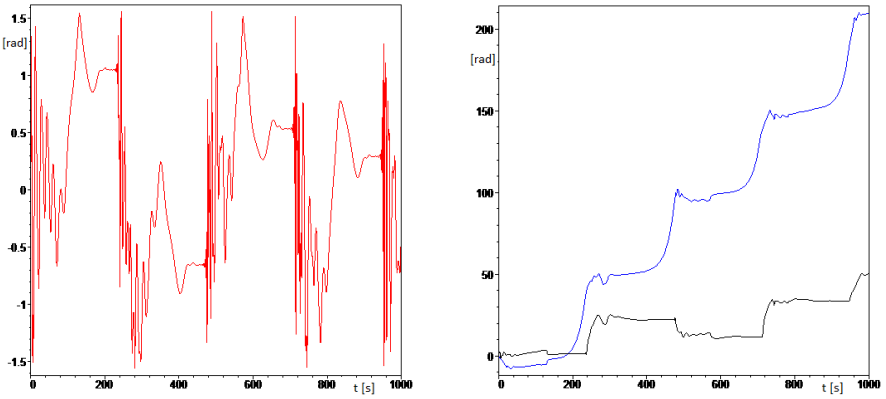

Fig. 29. The time-history of the angle $\gamma(t)$ (red), $\psi(t)$ (black), $\varphi(t)$ (blue) in the *Complex2* system

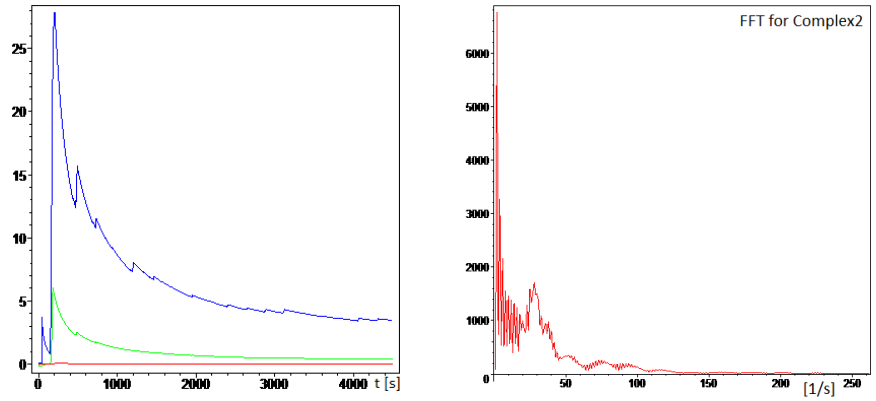

Fig. 30. The Lyapunov exponents and the spectrum of the fast Fourier transform of $x(t)$-signal

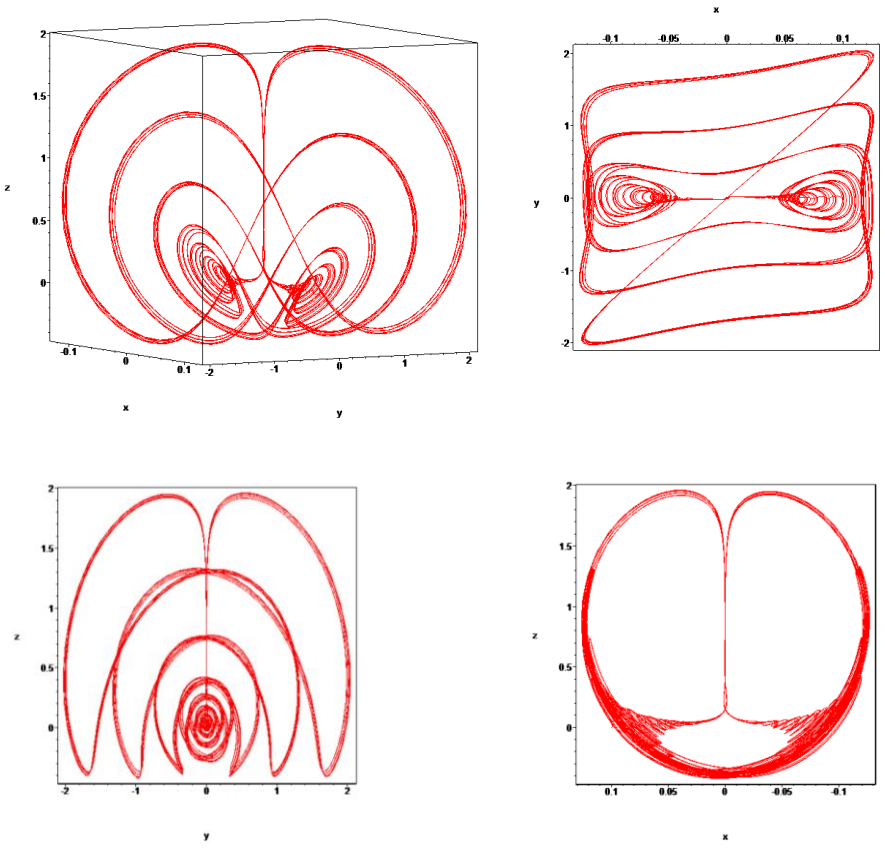

Fig. 31. Complex periodical cycle in the phase space of the *Complex2* system (in projections).

Conclusion

In this work the new dynamical systems of the Newton-Leipnik type with strange attractors (or with the complex dynamical behavior) were considered with the detailed numerical investigation of corresponding properties and with the evaluation of theirs characteristics. The phase spaces of the systems and generated strange attractors (and cycles) were explored, including the study of the main characteristics of chaotic/regular dynamics, such as the Lyapunov's exponents, the fractal dimension of strange attractors, the fast Fourier transform of the attractors' signals, the Poincaré sections. All of the considered dynamical systems have the "natural origin" corresponding to the mechanical and mathematical models of the angular motion of spacecraft; and, certainly, the results of the investigation can be applied to solving tasks of the spacecraft chaotic reorientation and chaotic maneuvering.

Acknowledgments This work is partially supported by the Russian Foundation for Basic Research (RFBR#15-08-05934-A), and by the Ministry of education and science of the Russian

Federation in the framework of the State Assignments to higher education institutions and research organizations in the field of scientific activity (the project # 9.1616.2017/ПЧ).

References

[1] A.V. Doroshin, New Strange Chaotic Attractors in Dynamical Systems of Multi-Spin Spacecraft and Gyrostats (2016) SAI Intelligent Systems Conference (IntelliSys-2016).

[2] A.V. Doroshin, Modeling of chaotic motion of gyrostats in resistant environment on the base of dynamical systems with strange attractors. Communications in Nonlinear Science and Numerical Simulation, Volume 16, Issue 8 (2011) 3188–3202.

[3] A.V. Doroshin, Initiations of Chaotic Regimes of Attitude Dynamics of Multi-Spin Spacecraft and Gyrostat-Satellites Basing on Multiscroll Strange Chaotic Attractors. SAI Intelligent Systems Conference (IntelliSys), London, U.K. (2015), 698 – 704.

[4] A.V. Doroshin, Multi-spin spacecraft and gyrostats as dynamical systems with multiscroll chaotic attractors. Science and Information Conference (SAI), London, U.K. (2014), 882 – 887.

[5] A.V. Doroshin, Initiations of chaotic motions as a method of spacecraft attitude control and reorientations (2016) IAENG Transactions on Engineering Sciences: pp. 15-28.

[6] R.B. Leipnik, T.A. Newton, Double strange attractors in rigid body motion with linear feedback control, Phys. Lett A 86 (1981) 63-67.

[7] Jafari, S., Sprott, J.C. & Nazarimehr, F. “Recent New Examples of Hidden Attractors”, The European Physical Journal Special Topics 224, (2015) 1469-1476.

[8] Z.Elhadj, J.C. Sprott, Simplest 3D continuous-time quadratic systems as candidates for generating multiscroll chaotic attractors, International Journal of Bifurcation and Chaos, Vol. 23, No. 7 (2013).

[9] Sprott, J. C. [1994] Some simple chaotic flows, Phys. Rev. E50.

[10] Sprott, J. C. [1997] Simplest dissipative chaotic flow, Phys. Lett. A 228, 271-274.

[11] Wang, Z., Sun, Y., van Wyk, B. J., Qi, G. & van Wyk, M. A. “A 3-D four-wing attractor and its analysis,” Brazilian J. Phys. 39, (2009) 547–553.

[12] Chen HK, Lee CI, Anti-control of chaos in rigid body motion. Chaos, Solitons & Fractals 2004; 21: 957-65.

[13] Sheu, L. J., Chen, H. K., Chen, J. H., Tam, L. M., Chen, W. C., Lin, K. T., & Kang, Y. (2008). Chaos in the Newton–Leipnik system with fractional order. Chaos, Solitons & Fractals, 36(1), 98-103.

[14] Wang, X., & Tian, L. (2006). Bifurcation analysis and linear control of the Newton–Leipnik system. Chaos, Solitons & Fractals, 27(1), 31-38.

[15] Jia, Q. (2008). Chaos control and synchronization of the Newton–Leipnik chaotic system. Chaos, Solitons & Fractals, 35(4), 814-824.

[16] Zhang, K., Wang, H., & Fang, H. (2012). Feedback control and hybrid projective synchronization of a fractional-order Newton–Leipnik system. Communications in Nonlinear Science and Numerical Simulation, 17(1), 317-328.

[17] Richter, H. (2002). Controlling chaotic systems with multiple strange attractors. Physics Letters A, 300(2), 182-188.

[18] Yun-Zhong, S., Guang-Zhou, Z., & Dong-Lian, Q. (2006). Passive control of chaotic system with multiple strange attractors. Chinese Physics, 15(10), 2266.

[19] Marlin, B. A. (2002). Periodic orbits in the Newton–Leipnik system. International Journal of Bifurcation and Chaos, 12(03), 511-523.